Preprints (www.preprints.org) | NOT PEER-REVIEWED | Posted: 19 August 2022 doi:10.20944/preprints202208.0354.v1

Weak Lensing, Hawking Radiation and Greybody Factor Bound by a Charged Black Holes with Nonlinear Electrodynamics Corrections

Wajiha Javed,[1,*] Mehak Atique,[1,†] Reggie C. Pantig,[2,‡] and Ali Övgün[3,§]
[1]*Department of Mathematics, Division of Science and Technology, University of Education, Lahore-54590, Pakistan*
[2]*Physics Department, De La Salle University, 2401 Taft Avenue, Manila, 1004 Philippines*
[3]*Physics Department, Eastern Mediterranean University, Famagusta, 99628 North Cyprus via Mersin 10, Turkey.*

In this work, we study gravitational lensing in the weak field limits and the shadow by charged black holes in non-linear electrodynamics corrections. To find the deflection angle in vacuum (non-plasma) up to the leading order terms, we compute the optical Gaussian curvature from optical metric and utilize the Gauss-Bonnet theorem by applying Gibbons and Werner's technique. Also, we derive the bending angle in plasma and dark matter mediums and observe that the bending angle increases by increasing the effects of these mediums. Further, in vacuum and plasma mediums, we investigate the graphical behavior of the bending angle with respect to the impact parameter u and notice that the bending angle exponentially decreases. Moreover, we calculate the Hawking temperature using the Gauss-Bonnet theorem and compare it with a standard method of computing the Hawking temperature. Furthermore, we investigate the bound of the greybody factor and graphically examine that bound converges to the 1. We relate our obtained results with the results of black holes given in the literature. Finally, we have considered exploring the effect of NLED, plasma, and dark matter on the black hole's shadow radius to broaden the study's scope. Results for the shadow indicate that the three parameters give different deviations to the shadow radius. Interestingly, while plasma affects both the photonsphere and shadow, dark matter only influences the shadow.

PACS numbers: 95.30.Sf, 98.62.Sb, 97.60.Lf
Keywords: general relativity; Gauss-Bonnet theorem; plasma medium; black hole; greybody; Hawking temperature; shadow cast

I. INTRODUCTION

From the beginning, studying black holes (BHs) has attracted scientific interest. In the general theory of relativity (GR), Einstein anticipated the existence of BHs. However, it was not until 1960 that the BHs were given the name we know today. The Event Horizon Telescope [1–3] took the first picture of the BH; before it, the picture of BH was only in simulations. A BH, by definition, is an area in spacetime where the gravitational pull is so powerful that nothing, including the light, can escape. A black hole has three layers the outer event horizon, inner event horizon, and singularity. There are three categories of BHs i.e., stellar BHs, supermassive BHs and intermediate BHs. The Schwarzschild, Reissner-Nordstrom, Kerr, and Kerr-Newman BHs are the four kinds of asymptotically flat BHs [4]. Schwarzschild BH is static that does not rotate and has no electric charge. This BH is characterized only by its mass. Kerr BH is a rotating BH with no electric charge, Reissner-Nordstrom is the charged and non-rotating BH, and Kerr-Newman BH is a charged and rotating BH. Black holes do not always stay the same type throughout their lives. Instead, they can become charged by attracting matter with higher positive or negative charges than the other, and they can lose their charge by attracting matter with lower positive or negative charges than the other. Similarly, BHs can attain angular momentum by absorbing matter in a non-spherically symmetric manner [4]. The existence of charged BHs has been discussed several times. In [5], it is discussed that a BH might have a little electric charge by assuming a balance between the number of protons and electrons around the BH. Moreover, the Wald [6] solution states that a revolving BH in a uniform magnetic field can still have an electric charge proportionate to its spin. While in the early universe, avoiding being neutralized by ordinary matter accreting on the magnetically charged BHs, these BHs are more likely to preserve their magnetic charge. [7].

Black holes are thought to have strong gravitational forces that prevent any radiation or particle from passing over the event horizon, absorbing everything in their vicinity. In 1974, in the background of quantum field theory, it was confirmed by Hawking that the BHs carry entropy and can generate a form of radiation known as Hawking radiation [8, 9]. The spectrum of BH radiation is the same as that of the black body. Since around the BH, spacetime is bent, the spectrum emitted by a BH has changed

*Electronic address: wajiha.javed@ue.edu.pk
†Electronic address: mehakatique1997@gmail.com
‡Electronic address: reggie.pantig@dlsu.edu.ph
§Electronic address: ali.ovgun@emu.edu.tr (corresponding author)

© 2022 by the author(s). Distributed under a Creative Commons CC BY license.

Preprints (www.preprints.org) | NOT PEER-REVIEWED | Posted: 19 August 2022 doi:10.20944/preprints202208.0354.v1

significantly. The curvature of spacetime can behave as a potential barrier, allowing some radiation to be transmitted and reflected. Accordingly, the greybody factor is determined by considering the transmission amplitude of BH radiation. The higher the magnitude of the greybody factor, the more likely Hawking radiation can approach to infinity.

Numerous strategies to probe the Hawking temperature were proposed [10–14]. To compute the hawking temperature for euclidean geometry of the 2-dimensional spacetime without losing the information of 4-dimensional spacetime, Robson et al. [15] proposed the topological method that is based on the invariants of the topology, i.e., Euler characteristic and Gauss-Bonnet theorem (GBT). Zhang et al.[16] studied the Hawking temperature of the BTZ BH using the topological approach. By utilizing the topological technique, Övgün et al. [17] attained the Hawking temperature for different BHs. Kruglov [18] investigated the Hawking temperature for a magnetically charged BH in the background of non-linear electrodynamics via surface gravity and horizon. Furthermore, a new method for computing the greybody factor that does not rely on approximations developed, which necessitates the determination of the bound of greybody factor. Some people use alternative approaches to find the greybody factor, including the WKB approximation and the matching methodology [13, 19–23]. For 1-dimensional potential scattering, Visser [24] established some extremely broad bounds for transmission and reflection coefficients. Boonserm and Visser [25] investigated the rigorous bounds of the greybody factor by analyzing the Regge-Wheeler equation for wave mode angular momentum and arbitrary particle spin for Schwarzschild BHs. Boonserm *et al.* [26] calculated the bounds for the greybody factor by considering the greybody factors related to the Myers-Perry BH scalar field excitation. For the greybody factor, authors [27] examined the bounds of the Kazakov Solodukhin BH.

In general, it is assumed that light travels in a straight path in a vacuum. In the context of Newtonian Mechanics, Soldner was the first to determine the deflection angle of light [28]. However, GR predicted that as the light travels through huge objects in the universe, it deflects because of the gravitational attraction of these objects, and the gravitational deflection of light by the Sun gave the first experimental evidence. This phenomenon is called gravitational lensing (GL) or "lensing". The GL in literature is classified into two regimes, strong and weak GLs relying on the alignment of the lens, and source [29–34]. Strong GL happens when the sightline from the viewer to the light source is so close to the lens. In this situation, the lens plane has a high magnification, multiple images, rings, and arcs. In contrast, the weak GL happens when the lens is far away from the sightline, producing mild image distortions and small magnifications. The GL by BHs has been extensively investigated in astronomy, and theoretical physics literature [35–39]. Gibbons and Werner (GW) [40, 41] demonstrated that in weak limits, it is feasible to determine the bending angle via GBT, and Werner then extended this approach to Kerr BHs via Nazim's osculating Riemannian mechanism with Randers-Finsler metric [42]. Gibbons and Werners struggle to developed a method to study the bending of light. In the Background of Einstein-Maxwell-dilation theory, authors [43] examined the bending of light by charged wormholes. Recently, it was studied how the GW approach may be utilized to compute the bending angle of a rotating global monopole spacetime [44], and for regular BHs with cosmic strings, [45]. Further, Ming et al. [46] investigated the weak lensing of electrically and magnetically charged BHs via the GW method in the context of non-linear electrodynamics. Many other authors have also utilized GW technique in [47–75].

In the GW approach, considering a region F_T bounded by a ray of light and the circular boundary curve D_T centered at the lens that meets the ray of light at the source and spectator, both of which are at a coordinate distance T from the lens. The GW technique indicates that the GBT is applied to the optical metric of the asymptotic spectator and source in the weak field limits given as

$$\int\int_{\mathcal{D}_T} \hat{\mathcal{K}} dS + \oint_{\partial \mathcal{D}_T} k dt + \sum_j \epsilon_j = 2\pi \mathcal{X}(\mathcal{D}_T), \tag{1}$$

where, $\hat{\mathcal{K}}$ stands for the optical Gaussian curvature and k is indicating the geodesic curvature, dS is the optical surface component, and at the jth vertex ϵ_j gives the exterior angle. The following equation can be used to calculate the asymptotic bending angle

$$\hat{\theta} = -\int_0^{\pi} \int_{r_{sl}}^{\infty} \hat{\mathcal{K}} dS, \tag{2}$$

where, $\hat{\theta}$ is representing the bending angle, summation of the jump angles $\sum_j \epsilon_j = \pi$ and Euler characteristic $\mathcal{X}(\mathcal{D}_T) = 1$. It is important to note that the integral is calculated over the infinite area of the surface bounded by the ray of light, not including the lens. Moreover, the straight line approximation (r_{sl}) will be used to compute the leading order term of the bending angle.

Dark matter (DM) was initially discovered by a Swiss astronomer named Zwicky [76]. Since DM cannot be observed directly, it was originally referred to as "missing matter." Dark matter comprises particles that do not reflect, absorb, or emit light and other forms of electromagnetic radiation. Dark matter consists of 27% of the total mass-energy of the universe [77]. Super-interacting massive particles, weakly interacting heavy particles, sterile neutrinos, and axions are different forms of DM candidates [78]. Dark matter has been proposed as a composite, similar to the dark atom idea, which can be examined using light deviation. Only gravitational interactions can identify DM, and we only know that DM is nonbaryonic, nonrelativistic, and has weak nongravitational interactions. The refractive index determines how fast a wave propagates across a medium. The refractive index

Preprints (www.preprints.org) | NOT PEER-REVIEWED | Posted: 19 August 2022 doi:10.20944/preprints202208.0354.v1

in the case of DM medium can be defined as [79]:

$$n(\omega) = 1 + \beta A_0 + A_2\omega^2 \tag{3}$$

Here, ω expresses the photon frequency. It is to be noticed here $\beta = \frac{\rho_0}{4m^2\omega^2}$, where ρ_0 is the mass density of dissipated DM particles, $A_0 = -2\varepsilon^2 e^2$ and $A_{2j} \geq 0$. Due to the usefulness of GL for dark matter detection Ovgun [68, 80, 81] studied the weak GL of wormholes and BHs in DM medium.

The problem of the singularity of an electric field in the origin of charged pointlike particles and the problem of infinite electromagnetic energy can be solved using non-linear electrodynamics (NLED). Non-linear electrodynamics may be transformed to Maxwell's electrodynamics, which can be regarded an approximation of Maxwell's electrodynamics at weak fields. The classical electrodynamics must be modified for strong electromagnetic fields because the self-interaction of photons is vital [82]. In the classic linear Maxwell theory, NLED was developed to solve the divergences in self-energy of pointlike charges. The Born and Infeld's NLED model was constructed to solve these divergences [83]. A fascinating feature of GR with NLED is that we can produce BHs without spacetime singularity, such as the Bardeen BH [84]. Various regular BHs have been produced as solutions in certain NLED theories [85–92].

Due to the GL of light, the area between the spectator and the BH is excluded from the definition of the BHs shadow, which is the spectator's dark sky without any light sources. A dark circular disc represents the shadow of a spherically symmetric BH. The Event Horizon Telescope Collaboration's [1, 93] experimental findings not only conclusively demonstrate the existence of BHs but also enable us to see BH shadows directly. Black hole shadows have been studied theoretically for a very long time. For the first time, Synge studied the shadows for Schwarzschild BHs [94] and later, Luminet [95] provided a formula for the shadow's angular radius. Generally, a revolving BH's shadow is longer than a non-rotating one due to spacetime dragging impacts, but a non-rotating spinning BH's shadow is frequently a conventional circle [96]. Gyulchev *et al.* [97]-[98] investigated the shadows formed by various traversable wormholes. It's interesting to note that the BHs shadow determines the geometry of the near horizon. However, the plasma around the BH impacts light's course. The Kerr geometry's shadow changes in geometric size and configuration as a result [99]. Dark matter, as an astrophysical environment, also leaves its signature on the black hole spacetime, and various researches went into this direction [100–105].

Inspired by these prior researches, we will examine the bending angle of a charged BH within NLED in the weak field approximations using the GBT. Further, it would be interesting to study the effect of plasma and DM mediums on the bending angle of light by a charged BH in the context of NLED. Moreover, we compute the Hawking temperature and greybody bound of the charged BH in the background of NLED. Graphical behavior will also be studied.

This paper is ordered as follows. In Sect. II, we discuss the charged BH within NLED. In Sect. III, we work for the bending angle of light within the vacuum and examine its graphical behavior. In Sect. IV, we study the deflection angle of light of BH in the presence of plasma medium and also observe the deflection angle graphically. In section Sect. V, we focus on the calculations of the deflection angle of BH in DM medium. Sect. VI is based on the calculations of the Hawking temperature of charged BH in NLED. In Sect. VII, we investigate the rigorous bound of the greybody factor of the charged BH and also discuss the graphical analysis of the bounds. Sect. VIII is based on the discussion of our findings. Natural units are also used as $G = c = 1$, and the metric signature is $(-,+,+,+)$ throughout the paper.

II. CHARGED BLACK HOLES IN NONLINEAR ELECTRODYNAMICS

The action of NLED in the general theory of relativity can be expressed as [106, 107],

$$S[g_{\mu\nu}, A_\mu] = \int d^4x\sqrt{-g}\left[\frac{R}{16\pi} - \mathcal{L}(\mathcal{F},\mathcal{G})\right], \tag{4}$$

where, $\mathcal{R}$ stands for the Ricci scalar computed from metric $g_{\mu\nu}$, $\mathcal{L}(\mathcal{F},\mathcal{G})$ is representing an arbitrary function in terms of $\mathcal{F}$ and $\mathcal{G}$, where $\mathcal{F} = \frac{1}{4}\mathcal{F}_{\mu\nu}\mathcal{F}^{\mu\nu}$ and $\mathcal{G} = \frac{1}{4}\mathcal{F}_{\mu\nu}\tilde{\mathcal{F}}^{\mu\nu}$. Here, $\mathcal{F}_{\mu\nu} = \partial_\mu A_\nu - \partial_\nu A_\mu$ is representing the strength field tensor of electromagnetic field and $\tilde{\mathcal{F}}_{\mu\nu} = \frac{1}{2}\epsilon_{\mu\nu ab}F^{ab}$ indicates the Hodge dual of $\mathcal{F}_{\mu\nu}$. Supposing that the Lagrangian in Eq. (4) is to be free of a cosmological constant. The spherically symmetric form of the magnetic field can be defined as

$$\frac{1}{2}\mathcal{F}_{\mu\nu}dx^\mu \wedge dx^\nu = qsin\theta d\theta \wedge d\phi, \tag{5}$$

where, q denotes the constant magnetic charge. The spherically symmetric solution is defined as [107]

$$ds^2 = g_{\mu\nu}dx^\mu dx^\nu = -f(r)dt^2 + \frac{1}{f(r)}dr^2 + r^2(d\theta^2 + sin^2\theta d\phi^2), \tag{6}$$

Preprints (www.preprints.org) | NOT PEER-REVIEWED | Posted: 19 August 2022 doi:10.20944/preprints202208.0354.v1

where

$$f(r) = 1 - \frac{2M}{r} + \frac{Q^2}{r^2} - \frac{\bar{\alpha} Q^2 M^4}{10 r^6}.$$

Here, in metric function $Q^2 = 4\pi q^2$ and a dimensionless parameter $\bar{\alpha}$ is $\frac{\alpha q^2}{M^4}$, constant M represents the mass of the gravitating body and α is the 4-dimensional parameter . One can observe that the metric in Eq. (6) takes the form of the Reissner-Nordstrom metric by considering $\bar{\alpha} = 0$. Also, the metric in Eq. (6) reduces to the Schwarzschild case by taking charge $Q = 0$.

III. BENDING ANGLE IN VACCUM

This section primarily focuses on the computation of the bending angle of charged BH within NLED using GBT with optical metrics given by GW. For this purpose, due to spherical symmetry, we utilize the equatorial plane $(\theta = \frac{\pi}{2})$ and null geodesics $(ds = 0)$ without affecting generality. The spacetime can be reduced to the orbital plane rays of light, i.e.,

$$dt^2 = g_{ab} dx^a dx^b = \frac{1}{(f(r))^2} dr^2 + \frac{r^2}{f(r)} d\phi^2, \tag{7}$$

where g_{ab} is the optical metric and $a, b \in \{1, 2\}$. Now, we calculate the non-zero Christoffel symbols of the optical metric as

$$\tilde{\Gamma}^r_{rr} = \frac{-20Mr^5 + Q^2\left(20r^4 - 6M^4\bar{\alpha}\right)}{10r^6(-2M + r) + Q^2\left(10r^5 - M^4 r\bar{\alpha}\right)},$$

$$\tilde{\Gamma}^r_{\phi\phi} = 3M - \frac{2Q^2}{r} - r + \frac{2M^4 Q^2 \bar{\alpha}}{5r^5},$$

$$\tilde{\Gamma}^r_{r\phi} = \frac{10r^5(-3M + r) + 4Q^2\left(5r^4 - M^4\bar{\alpha}\right)}{10r^6(-2M + r) + Q^2\left(10r^5 - M^4 r\bar{\alpha}\right)}.$$

We work out for the Ricci scalar by utilizing the above non-zero Christoffel symbols of the optical metric to calculate the Gaussian optical curvature. The Ricci scalar can be computed as

$$\begin{aligned}\mathcal{R} &= \frac{4Q^4}{r^6} - \frac{12MQ^2}{r^5} + \frac{6M^2}{r^4} + \frac{6Q^2}{r^4} - \frac{4M}{r^3} - \frac{18M^4Q^4\bar{\alpha}}{5r^{10}} \\ &+ \frac{38M^5Q^2\bar{\alpha}}{5r^9} - \frac{21M^4Q^2\bar{\alpha}}{5r^8} + \frac{6M^8Q^4\bar{\alpha}^2}{25r^{14}}.\end{aligned} \tag{8}$$

The Gaussian curvature of the optical metric of the charged BH within NLED can be computed by utilizing the following relation

$$\hat{\mathcal{K}} = \frac{R}{2}. \tag{9}$$

By using the value of $\mathcal{R}$ in Eq.((9)), the optical Gaussian curvature up to the leading order terms is calculated as

$$\hat{\mathcal{K}} \simeq \frac{3Q^2}{r^4} - \frac{2M}{r^3} - \frac{6Q^2M}{r^5} + \frac{3M^2}{r^4} - \frac{21\bar{\alpha}Q^2M^4}{10r^8} + \mathcal{O}(M^5, Q^3, \bar{\alpha}^2). \tag{10}$$

The bending angle $\hat{\theta}$ will be computed using the result above. One can notice that the Gaussian optical curvature $\hat{\mathcal{K}}$ is in the direct relation with the mass m, charge Q and parameter $\bar{\alpha}$, but this information is nothing to do with our work. Consider D_T to be a non-singular region of an orientated 2-dimensional surface S with the optical metric and boundaries $\partial D_T = \gamma_g \cup F_T$. Considering the Gaussian optical curvature and geodesic curvature, the Gauss-Bonnet Theorem is then written as follows in terms of the construction above [41]:

$$\int\int_{\mathcal{D}_T} \hat{\mathcal{K}} dS + \oint_{\partial \mathcal{D}_T} k dt + \sum_j \epsilon_j = 2\pi \mathcal{X}(\mathcal{D}_T). \tag{11}$$

Preprints (www.preprints.org) | NOT PEER-REVIEWED | Posted: 19 August 2022 doi:10.20944/preprints202208.0354.v1

The regular domain in the optical plane is selected to be outside of the light beam. This domain is assumed to have the topology of a disc with the Euler characteristic number $\mathcal{X}(\mathcal{D}_T) = 1$. Taking start with a smooth curve described as $\gamma := \{t\} \to D_T$, with the geodesic curvature determined as follows:

$$k = g(\nabla_{\dot{\gamma}}\dot{\gamma}, \ddot{\gamma}). \tag{12}$$

In addition, the condition of unit speed is $g(\dot{\gamma}, \dot{\gamma}) = 1$, where $\ddot{\gamma}$ indicates the unit acceleration vector. Now, take a very large but finite radial distance $T \to \infty$, so that two jump angles at the source and viewer give $\theta_S + \theta_O \to \pi$. It is noted that the geodesic curvature for the beam of light γ_g eliminates by definition $k(\gamma_g) = 0$. By computing only the contribution to the curve F_T and we may deduce the following result from GBT

$$\lim_{T\to\infty} \int_0^{\pi+\hat{\theta}} \left[k\frac{dt}{d\phi}\right]_{F_T} d\phi = \pi - \lim_{T\to\infty} \int\int_{D_T} \hat{\mathcal{K}} dS. \tag{13}$$

The geodesic curvature for a curve F_T placed at a T (coordinate distance) from the coordinate system can be determined as

$$k(F_T) = \mid \nabla_{\dot{F}_T}\dot{F}_T \mid . \tag{14}$$

The radial component for geodesic curvature is specified as [41]

$$(\nabla_{\dot{F}_T}\dot{F}_T)^r = \dot{F}_T^{\phi}(\partial_{\phi}\dot{F}_T^r) + \tilde{\Gamma}^r_{\phi\phi}(\dot{F}_T^{\phi})^2. \tag{15}$$

The unit speed condition and optical metric of charged BH can be used to demonstrate that

$$\lim_{T\to\infty} k(F_T) = \lim_{T\to\infty} \mid \nabla_{\dot{F}_T}\dot{F}_T \mid = \frac{1}{T}. \tag{16}$$

On the other hand, from the charged BH's optical metric, we obtain

$$\lim_{T\to\infty} dt \to T d\phi. \tag{17}$$

We may conclude that our charged BH optical metric is asymptotically Euclidean. By combining the above two equations, we get

$$\lim_{T\to\infty} \left(k(F_T)\frac{dt}{d\phi}\right) = 1. \tag{18}$$

Using Eq.(13) and the straight line approximation, $r = \frac{u}{\sin\phi}$, where, u is the impact parameter. The bending angle $\hat{\theta}$ can be defined as

$$\hat{\theta} = -\int_0^{\pi}\int_{\frac{u}{\sin\phi}}^{\infty} \hat{\mathcal{K}} dS, \tag{19}$$

where $dS = \sqrt{detg}drd\phi$. Now by using the Eqs.(10) and (19), the bending angle $\hat{\theta}$ of the charged BH up to the leading order terms is calculated as

$$\begin{aligned}\hat{\theta} \simeq\ & \frac{4M}{u} + \frac{8M^3}{3u^3} + \frac{3M^2\pi}{4u^2} + \frac{75M^4\pi}{64u^4} \\ & - \frac{8MQ^2}{3u^3} - \frac{8M^3Q^2}{u^5} - \frac{3\pi Q^2}{4u^2} - \frac{45M^2\pi Q^2}{32u^4} \\ & - \frac{1225M^4\pi Q^2}{256u^6} + \frac{7M^4\pi Q^2\bar{\alpha}}{64u^6} + \mathcal{O}(M^5, Q^3, \bar{\alpha}^2).\end{aligned} \tag{20}$$

The attained angle Eq. (20) depends on the mass M of a gravitating body, charge Q, dimensionless parameter $\bar{\alpha}$ and the impact parameter u. We examine that by ignoring the term which contains $\bar{\alpha}$ in obtained angle, one can get the deflection angle of Reissner-Nordstrom BH. We also observe that by neglecting charge Q in bending angle Eq. (20) one can obtain the deflection angle of the Schwarzschild BH up to the fourth order of mass M in vacuum.

Preprints (www.preprints.org) | NOT PEER-REVIEWED | Posted: 19 August 2022 doi:10.20944/preprints202208.0354.v1

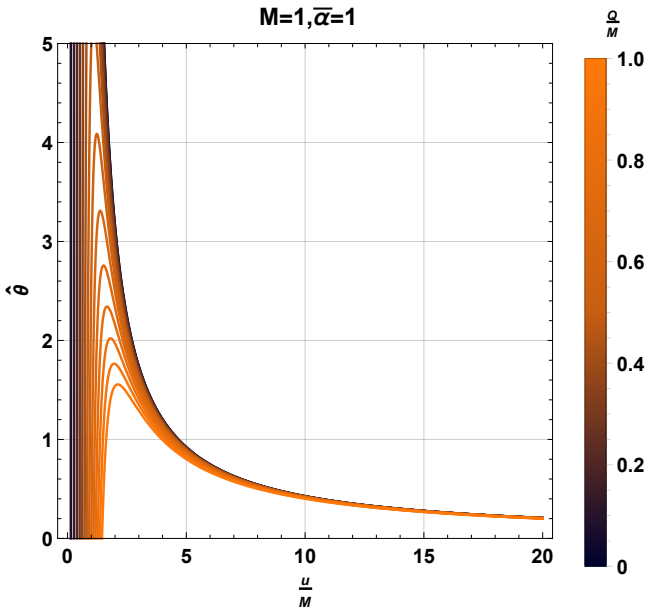

FIG. 1: The variation of the bending angle $\hat{\theta}$ as a function of impact parameter u.

A. Graphical behavior in Vaccum

This subsection focuses primarily on a graphical analysis of BH's angle of deflection $\hat{\theta}$ with respect to the impact parameter u in non-plasma medium for the various values of Q by taking M and $\bar{\alpha}$ equal to 1 and $0 \leq u \leq 20$. Fig. 1 depicts the behavior of bending angle $\hat{\theta}$ with respect to impact parameter u for $0 \leq Q \leq 1$. We find that for the small values of u, the bending angle $\hat{\theta}$ is positive. The bending angle $\hat{\theta}$ approaches zero as the values of u increase. We also inspect that bending angle $\hat{\theta}$ obtains its maximum value and then exponentially decreases as the value of charge increases $Q \to 1$. For $Q = 0$, one can get the behavior of the Schwarzschild BH's bending angle (indicated by the black line), i.e., exponentially decreases and approaches zero. The positive angle at these values of Q indicates the deflection is in the upward direction. The behavior of bending angle $\hat{\theta}$ is physically stable.

IV. PLASMA'S IMPACT ON BENDING ANGLE

This section aims to investigate the plasma medium's effect on the bending angle $\hat{\theta}$. In a vacuum, lensing does not include the photon's dispersive properties, while in a plasma medium, gravitational deflection causes refraction to include additional deflection, which encodes the information in the refraction index. [108]. To account for the impacts of plasma, we assume the photon goes from vacuum to a hot, ionized gas medium, with v equal to the speed of light through the plasma. The refractive index, $n(r)$, may therefore be stated as follows:

$$n(r) = \frac{v}{c} = \frac{1}{dr/dt}, \quad \text{where} \quad c = 1. \tag{21}$$

The refractive index for the charged BH within NLED is obtained as [89]

$$n(r) = \sqrt{1 - \frac{\omega_e^2}{\omega_\infty^2}(f(r))}, \tag{22}$$

where, in refractive index ω_e and ω_∞ stand for the electron plasma frequency and photon frequency, respectively, observed from infinity by a spectator. Considering, a 2-dimensional Riemannian manifold $(M^{opt}; g_{kl}^{opt})$ with the optical metric $g_{kl}^{opt} = -\frac{n^2}{g_{11}} g_{kl}$.

Preprints (www.preprints.org) | NOT PEER-REVIEWED | Posted: 19 August 2022 doi:10.20944/preprints202208.0354.v1

Then, the line-element in Eq. (6) in the optical space Eq. (7) in the case of plasma medium takes the form

$$dt^2 = g^{opt}_{kl}dx^k dx^l = n^2\left[\frac{dr^2}{f^2(r)} + \frac{r^2 d\phi^2}{f(r)}\right]. \tag{23}$$

The non-zero Christoffel symbols of the charged BH in case of plasma medium by using the components of metric Eq. (23) is calculated as

$$\tilde{\Gamma}^r_{rr} = \frac{(f(r)\omega_e^2 - 2\omega_\infty^2)(f(r)\omega_e^2 + \omega_\infty^2)f'(r)}{2f(r)\omega_\infty^4},$$

$$\tilde{\Gamma}^r_{r\phi} = \frac{r}{2}\left(\frac{(f(r))^3\omega_e^4}{\omega_\infty^4} + rf'(r) - 2f(r) + \frac{r\omega_e^2 f'(r)}{\omega_\infty^2}f(r)\right),$$

$$\tilde{\Gamma}^r_{\phi\phi} = \frac{1}{r} - \frac{(f(r))^2\omega_e^4}{r\omega_\infty^4} - \frac{f'(r)}{2f(r)}.$$

The Gaussian optical curvature $\hat{\mathcal{K}}$ for charged BH in the case of plasma medium is calculated by using the relation in Eq. (9)

$$\begin{aligned}\hat{\mathcal{K}} \simeq\ & \frac{3Q^2}{r^4} + \frac{5Q^2\omega_e^2}{r^4\omega_\infty^2} - \frac{2M}{r^3} - \frac{3M\omega_e^2}{r^3\omega_\infty^2} - \frac{6MQ^2}{r^5} \\ & - \frac{26MQ^2\omega_e^2}{r^5\omega_\infty^2} + \frac{3M^2}{r^4} + \frac{12M^2\omega_e^2}{r^4\omega_\infty^2} + \frac{32Q^2M^2\omega_e^2}{r^6\omega_\infty^2} - \frac{12M^3\omega_e^2}{r^5\omega_\infty^2} \\ & - \frac{21\bar{\alpha}Q^2M^4}{10r^8} - \frac{39Q^2M^4\bar{\alpha}\omega_e^2}{10r^8\omega_\infty^2} + \mathcal{O}(M^5, Q^3, \bar{\alpha}^2).\end{aligned} \tag{24}$$

From the above result, one can observe that the Gaussian optical curvature $\hat{\mathcal{K}}$ also directly relates to the electron plasma frequency and inverse with photon frequency. With the help of GBT given in Eq. (19), one can calculate the bending angle $\hat{\theta}$ of the charged BH within the plasma medium as

$$\begin{aligned}\hat{\theta} \simeq\ & \frac{4M}{u} + \frac{8M^3}{3u^3} + \frac{3M^2\pi}{4u^2} + \frac{75M^4\pi}{64u^4} \\ & - \frac{8MQ^2}{3u^3} - \frac{8M^3Q^2}{u^5} - \frac{3\pi Q^2}{4u^2} - \frac{45M^2\pi Q^2}{32u^4} \\ & - \frac{1225M^4\pi Q^2}{256u^6} + \frac{7M^4\pi Q^2\bar{\alpha}}{64u^6} - \frac{Q^2\pi\omega_e^2}{2u^2\omega_\infty^2} + \frac{2M\omega_e^2}{u\omega_\infty^2} + \frac{2Q^2M\omega_e^2}{u^3\omega_\infty^2} \\ & - \frac{M^2\pi\omega_e^2}{2u^2\omega_\infty^2} + \frac{3M^2Q^2\pi\omega_e^2}{8u^4\omega_\infty^2} - \frac{2G^3M^3\omega_e^2}{3u^3\omega_\infty^2} + \frac{4M^3Q^2\omega_e^2}{3u^5\omega_\infty^2} \\ & - \frac{3M^4\pi\omega_e^2}{16u^4\omega_\infty^2} + \frac{75M^4\pi\omega_e^2}{128u^6\omega_\infty^2} \\ & + \frac{3M^4\pi Q^2\bar{\alpha}\omega_e^2}{32u^6\omega_\infty^2} + \mathcal{O}(M^5, Q^3, \bar{\alpha}^2).\end{aligned} \tag{25}$$

The bending angle obtained in Eq. (25) depends on the mass M of a gravitating body, charge Q, dimensionless parameter $\bar{\alpha}$, impact parameter u and plasma terms. We also observe that the angle in Eq. (25) in the absence of plasma effect reduces to the angle (20). By considering $\bar{\alpha} = 0$, the angle reduces to the deflection angle of Reissner-Nordstrom BH up to the fourth order of M in plasma medium. The bending angle $\hat{\theta}$ of the charged BH reduces to the bending angle of Schwarzschild BH by considering $Q = 0$. It is to be observed that the bending in plasma medium angle Eq. (25) is greater than the case without plasma effect. The deflection angle $\hat{\theta}$ increases as the photon frequency viewed by a static observer at infinity decreases, keeping the electron plasma frequency constant.

Preprints (www.preprints.org) | NOT PEER-REVIEWED | Posted: 19 August 2022 doi:10.20944/preprints202208.0354.v1

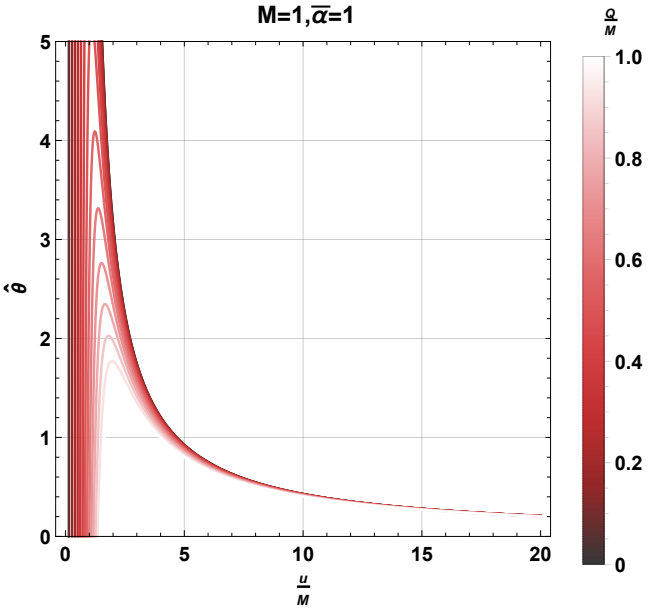

FIG. 2: The variation of the bending angle $\hat{\theta}$ as a function of impact parameter u

.

A. Graphical behavior in Plasma Medium

This subsection aims to study the graphical analysis of BH's deflection angle $\hat{\theta}$ with respect to the impact parameter u in plasma medium for various values of Q by taking M and $\bar{\alpha}$ equal to 1, $0 \leq u \leq 20$ and $\frac{\omega_e}{\omega_\infty} = 0.1$. Fig. 2 depicts the behavior of the bending angle $\hat{\theta}$ with respect to the impact parameter u for $0 \leq Q \leq 1$. We examine that for the small values of u, the bending angle $\hat{\theta}$ is positive. The bending angle $\hat{\theta}$ approaches zero as the values of u increase. We also inspect that bending angle $\hat{\theta}$ obtained its maximum value and then exponentially decreases as the values of charge increase $Q \to 1$. For $Q = 0$, one can get the behavior of the Schwarzschild BH's bending angle (indicated by the black line) i.e. exponentially decreases and goes to zero. One can attain the positive angle for these values of Q, which indicates that the deflection is in the upward direction. The behavior of bending angle $\hat{\theta}$ is physically stable. One can observe that the bending angle $(\hat{\theta})$ graphically shows a similar behavior in both mediums.

V. BENDING ANGLE IN DARK MATTER MEDIUM

Sect. In this section, we will compute the deflection angle of a ray of light propagating through a charged BH embedded in a DM medium with various configurations of the BH. In this regard, the refractive index for the charged BH in the DM medium is defined as [109]

$$n(\omega) = 1 + \beta A_0 + A_2\omega^2. \tag{26}$$

The 2-dimensional optical geometry of the charged BH within NLED is defined in Eq. (23). Now, by using the value of the refractive index in (26), the Gaussian optical curvature $\hat{\mathcal{K}}$ of the charged BH in terms of DM medium is calculated as

$$\begin{aligned}\hat{\theta} \simeq & \frac{3Q^2}{r^4(1+A_2\omega^2+A_0\beta)^2} - \frac{2M}{r^3(1+A_2\omega^2+A_0\beta)^2} - \frac{6MQ^2}{r^5(1+A_2\omega^2+A_0\beta)^2} \\ & + \frac{3M^2}{r^4(1+A_2\omega^2+A_0\beta)^2} - \frac{21\bar{\alpha}M^4Q^2}{10r^8(1+A_2\omega^2+A_0\beta)^2} + \mathcal{O}(M^5, Q^3, \bar{\alpha}^2).\end{aligned} \tag{27}$$

Preprints (www.preprints.org) | NOT PEER-REVIEWED | Posted: 19 August 2022 doi:10.20944/preprints202208.0354.v1

Using Eq.(19), the bending angle can be computed as

$$\begin{aligned}\hat{\theta} \simeq & \frac{4M}{u(1+A_2\omega^2+A_0\beta)^2}+\frac{8M^3}{3u^3(1+A_2\omega^2+A_0\beta)^2} \\ & +\frac{3M^2\pi}{4u^2(1+A_2\omega^2+A_0\beta)^2}+\frac{75M^4\pi}{64u^4(1+A_2\omega^2+A_0\beta)^2} \\ & -\frac{8MQ^2}{3u^3(1+A_2\omega^2+A_0\beta)^2}-\frac{8M^3Q^2}{u^5(1+A_2\omega^2+A_0\beta)^2} \\ & -\frac{3\pi Q^2}{4u^2(1+A_2\omega^2+A_0\beta)^2}-\frac{45M^2\pi Q^2}{32u^4(1+A_2\omega^2+A_0\beta)^2} \\ & -\frac{1225M^4\pi Q^2}{256u^6(1+A_2\omega^2+A_0\beta)^2}+\frac{7M^4\pi Q^2\bar{\alpha}}{64u^6(1+A_2\omega^2+A_0\beta)^2} \\ & +\frac{3M^2\pi A_2\omega^2}{2u^2(1+A_2\omega^2+A_0\beta)^2}+\frac{75M^4\pi A_2\omega^2}{32u^4(1+A_2\omega^2+A_0\beta)^2} \\ & -\frac{16GMQ^2A_2\omega^2}{3u^3(1+A_2\omega^2+A_0\beta)^2}-\frac{16M^3Q^2A_2\omega^2}{u^5(1+A_2\omega^2+A_0\beta)^2} \\ & -\frac{3\pi Q^2A_2\omega^2}{2u^2(1+A_2\omega^2+A_0\beta)^2}-\frac{45M^2\pi Q^2A_2\omega^2}{16u^2(1+A_2\omega^2+A_0\beta)^2} \\ & -\frac{1225M^4\pi Q^2A_2\omega^2}{128u^6(1+A_2\omega^2+A_0\beta)^2}+\frac{8MA_2\omega^2}{u(1+A_2\omega^2+A_0\beta)^2} \\ & +\frac{16M^3A_2\omega^2}{3u^3(1+A_2\omega^2+A_0\beta)^2}+\mathcal{O}(M^5,Q^3,\bar{\alpha}^2,\omega^4). \end{aligned} \tag{28}$$

The bending angle in Eq. (28) depends on the mass M of a gravitating body, charge Q, dimensionless parameter $\bar{\alpha}$, impact parameter u and DM terms. Thus, one can obtain the expression for Reissner-Nordstrom BH's deflection angle by taking $\bar{\alpha}=0$ and for the Schwarzschild BH by considering $Q=0$ in DM medium. Due to the DM's effect, we examine that the deflection angle of the charged BH is larger than the angle obtained in vacuum. The deflection angle in Eq. (28) reduces to the deflection angle in Eq. (20) obtained in a vacuum by ignoring the effect of the DM medium.

VI. HAWKING RADIATION

The main aim of this section is to calculate the Hawking radiation of charged BH within NLED via a topological method. The topological technique uses the 2-dimensional Euler characteristic and GBT to compute the BH temperature. For this, the spherically symmetric solution can be defined as [107]

$$ds^2=-f(r)dt^2+\frac{1}{f(r)}dr^2+r^2(d\theta^2+sin^2\theta d\phi^2). \tag{29}$$

By utilizing the Wick rotation, we can rewrite the 4-dimensional spherically symmetric metric into 2-dimensional as

$$ds^2=-f(r)dt^2+\frac{1}{f(r)}dr^2. \tag{30}$$

The event horizon r_h of the charged BH in NLED is defined as

$$\begin{aligned} r_h = & GM+\sqrt{(M)^2-Q^2} \\ & +\bar{\alpha}Q^2M^4\Big(20(M+\sqrt{M^2-Q^2})^3((M \\ & +\sqrt{(M)^2-Q^2})M-Q^2)\Big)^{-1}+\mathcal{O}(\bar{\alpha}^2). \end{aligned} \tag{31}$$

Preprints (www.preprints.org) | NOT PEER-REVIEWED | Posted: 19 August 2022 doi:10.20944/preprints202208.0354.v1

The formula to compute the Hawking temperature of the charged BH in NLED is defined as follows [15, 17]

$$T_H = \frac{\hbar c}{4\pi \mathcal{X} k_B} \sum_{j \leq \mathcal{X}} \int_{r_{h_i}} \sqrt{g} \mathcal{R} dr, \tag{32}$$

where, $\hbar$ represents the Plank constant, c indicates the speed of light, k_B is the Boltzmann's constant, g is the determinant of the 2-dimensional metric. Besides, r_h indicates the horizon with ith Killing horizon. For simplicity, we consider all physical constants equal to unity. After putting the values of all the constants, we get

$$T_H = \frac{1}{4\pi \mathcal{X}} \int_{r_h} \sqrt{g} \mathcal{R} dr, \tag{33}$$

while, the value of g is 1 and the Ricci scalar R is calculated as

$$\mathcal{R} = \frac{4M}{r^3} - \frac{6Q^2}{r^4} + \frac{21M^4Q^2\bar{\alpha}}{5r^8}. \tag{34}$$

After putting the Ricci scalar, and the determinant of metric and then taking integration along the horizon, the Hawking temperature of the charged BH in NLED is computed as

$$\begin{aligned} T_H &= \frac{3M^4Q^2\bar{\alpha}}{20\pi} \left(M + \sqrt{\psi} + \frac{M^4Q^2\bar{\alpha}}{20(M+\sqrt{\psi})^3(M(M+\sqrt{\psi}) - Q^2)} \right)^{-7} \\ &- \frac{2Q^2}{4\pi} \left(M + \sqrt{\psi} + \frac{M^4Q^2\bar{\alpha}}{20(M+\sqrt{\psi})^3(M(M+\sqrt{\psi}) - Q^2)} \right)^{-3} \\ &+ \frac{2M}{4\pi} \left(M + \sqrt{\psi} + \frac{M^4Q^2\bar{\alpha}}{20(M+\sqrt{\psi})^3(M(M+\sqrt{\psi}) - Q^2)} \right)^{-2}, \end{aligned} \tag{35}$$

where, $\psi = M^2 - Q^2$. One can observe that the obtained Hawking temperature in Eq. (35) depends on the M, Q, and $\bar{\alpha}$. We also examine that the Hawking Temperature derived via GBT is identical to the standard form of deriving the Hawking temperature using horizon function ($T_H = \frac{f'(r_h)}{4\pi}$). By taking $\bar{\alpha} = 0$, the Hawking temperature of Reissner-Nordstrom BH can be obtained, and by considering $Q = 0$, one can get the Hawking temperature of Schwarzschild BH ($T_H = \frac{1}{8M\pi}$).

VII. BOUNDING GREYBODY FACTOR

In this section, we examine the rigorous bound of the greybody factor of charged BH in NLED. The spherically symmetric metric of the charged BH in NLED is given in Eq. (6) and the corresponding greybody factor bound can be written as [25]

$$T \geq Sech^2 \left(\frac{1}{2\omega} \int_{-\infty}^{\infty} \varrho dr_* \right), \tag{36}$$

where

$$\varrho = \frac{\sqrt{[h'(r_*)]^2 + [\omega^2 - \tilde{\mathcal{V}}(r_*) - h^2(r_*)]^2}}{2h(r_*)},$$

where, $h(r_*)$ representing the positive function satisfies the condition $h(-\infty) = h(+\infty) = \omega$. The Schrödinger-like equation in terms of the tortoise coordinate r_* takes the following form

$$\left[\frac{d^2}{dr_*^2} - \omega^2 + \tilde{\mathcal{V}}(r) \right] \psi = 0, \tag{37}$$

here, $dr_* = \frac{1}{f(r)} dr$ and $\tilde{\mathcal{V}}(r)$ indicates potential and is defined as

$$\tilde{\mathcal{V}}(r) = f(r) \left[\frac{f'(r)}{r} + \frac{l(l+1)}{r^2} \right]. \tag{38}$$

Preprints (www.preprints.org) | NOT PEER-REVIEWED | Posted: 19 August 2022 doi:10.20944/preprints202208.0354.v1

The potential for the charged BH in NLED is calculated as

$$\tilde{\mathcal{V}}(r) = \left(1 + \frac{Q^2}{r^2} - \frac{2M}{r} - \frac{M^4Q^2\bar{\alpha}}{10r^6}\right)\left[\frac{l(1+l)}{r^2} + \frac{\left(-\frac{2Q^2}{r^3} + \frac{2M}{r^2} + \frac{3M^4Q^2\bar{\alpha}}{5r^7}\right)}{r}\right] \tag{39}$$

The lower bound on the transmission probability T for $h = \omega$ is defined as

$$T \geq Sech^2\left(\frac{1}{2\omega}\int_{r_h}^{\infty}\frac{\tilde{\mathcal{V}}(r)}{f(r)}dr\right). \tag{40}$$

The greybody bound by charged BH within NLED after putting the value of $\tilde{\mathcal{V}}(r)$ in Eq.(40) and using the value of horizon, the bound can be evaluated as

$$\begin{aligned} T \geq\ & Sech^2\left[\frac{3M^4Q^2\bar{\alpha}}{70\omega}\left(M + \sqrt{\psi} + \frac{M^4Q^2\bar{\alpha}}{20(M+\sqrt{\psi})^3(M(M+\sqrt{\psi}) - Q^2)}\right)^{-7}\right. \\ & - \frac{Q^2}{3\omega}\left(M + \sqrt{\psi} + \frac{M^4Q^2\bar{\alpha}}{20(M+\sqrt{\psi})^3(M(M+\sqrt{\psi}) - Q^2)}\right)^{-3} \\ & + \frac{M}{2\omega}\left(M + \sqrt{\psi} + \frac{M^4Q^2\bar{\alpha}}{20(M+\sqrt{\psi})^3(M(M+\sqrt{\psi}) - Q^2)}\right)^{-2} \\ & \left. + \frac{l(l+1)}{2\omega}\left(M + \sqrt{\psi} + \frac{M^4Q^2\bar{\alpha}}{20(M+\sqrt{\psi})^3(M(M+\sqrt{\psi}) - Q^2)}\right)^{-1}\right]. \end{aligned} \tag{41}$$

where, $\psi = M^2 - Q^2$. The obtained bound in Eq. 41) depends on the M, Q and $\bar{\alpha}$. By considering $\bar{\alpha} = 0$, one can also get the expression of Reissner-Nordstrom BH's greybody bound, and by taking $Q = 0$, the greybody bound of Schwarzschild BH's can be attained.

A. Graphical Analysis of Greybody Bound

This part depicts the graphical behavior of the bound of greybody factor and the potential (we set $\tilde{\mathcal{V}}(r) = V(r)$) of charged BH within NELD for the different values of charge Q, and taking angular momentum $l = 0, 1, 2$.

Fig. 3 we examine that for $l = 0$ and $0 \leq Q \leq 1$ potential decreases and becomes zero as far as r increases, and the corresponding bound increases and remains 1 as the value of ω approaches the infinity. Fig. 4, we examine that the potential with value $l = 1$ and $0 \leq Q \leq 1$ exponentially decreases and approaches zero as far as r increases, and the corresponding bound increases as the value of ω approaches infinity and shows the convergent behavior by converging to 1. Fig. 5, It is to be mentioned here that for $l = 2$ the potential and the greybody bound show a similar behavior as for $l = 1$.

VIII. SHADOW CAST BEHAVIOR

In this section, we will investigate the shadow behavior of the charged black hole in non-linear electrodynamics and how it is influenced by plasma or the dark matter refractive index, as mentioned in this study. We know that a non-spinning black hole produces a shadow that is a perfect circle. While it is instructive to plot it, a line plot of the shadow radius curve will give us more information about its behavior based on where the observer is located relative to the black hole.

The Hamiltonian for light rays, with the non-magnetized cold plasma frequency $\omega_p(r)$ [110], is given as

$$H = \frac{1}{2}g^{ik}p_ip_k = \frac{1}{2}\left(-\frac{p_t^2}{A(r)} + \frac{p_r^2}{B(r)} + \frac{p_\phi^2}{C(r)} + \omega_p(r)^2\right). \tag{42}$$

In this equation, we will analyze plasma's influence as perceived by a static observer at r_{obs} and $\theta_{obs}\pi/2$, which is chosen since the metric has spherical symmetry along t and phi coordinates. Due to this, the equations of motion (EoS) can be derived through

Preprints (www.preprints.org) | NOT PEER-REVIEWED | Posted: 19 August 2022 doi:10.20944/preprints202208.0354.v1

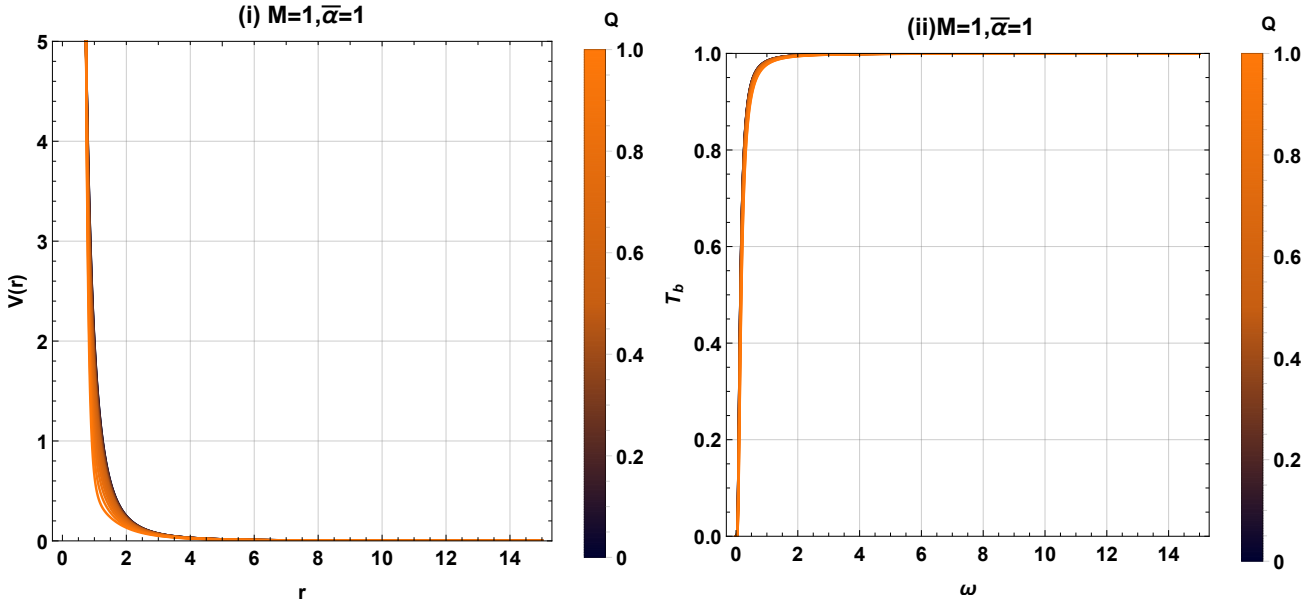

FIG. 3: The potential with $l = 0$ is shown in (i), and the corresponding bound of greybody factor of charged BH is shown in (ii).

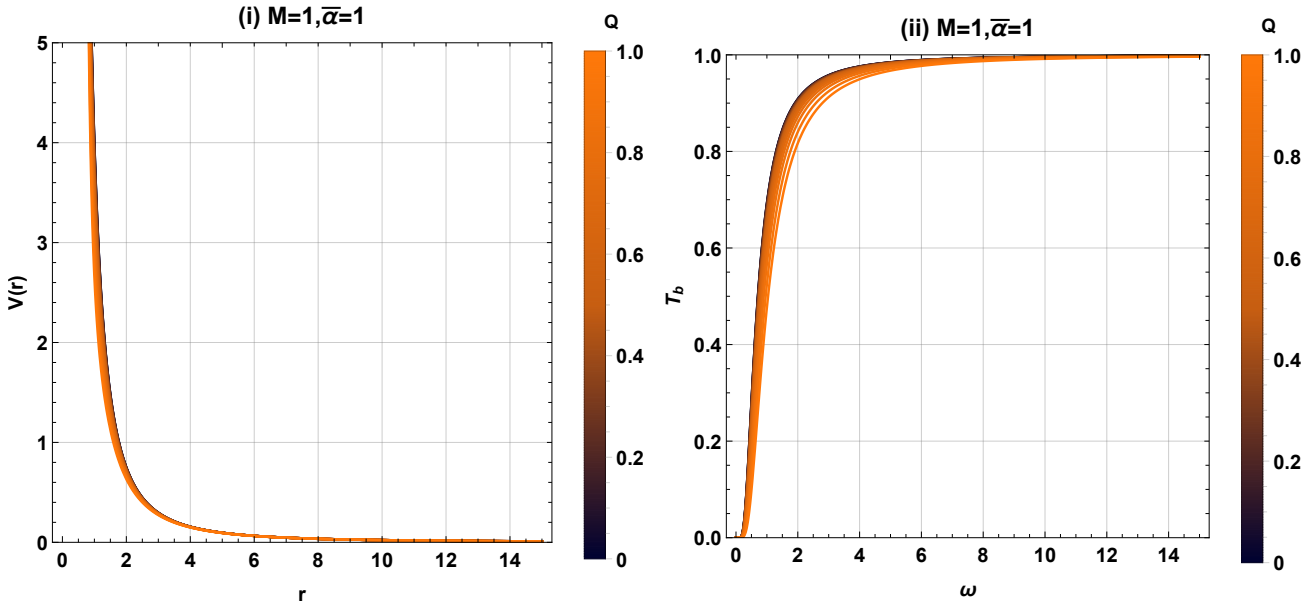

FIG. 4: The potential with $l = 1$ is shown in (i), and the corresponding bound of greybody factor of charged BH is shown in (ii).

the following:

$$\dot{x}^i = \frac{\partial H}{\partial p_i}, \qquad \dot{p}_i = -\frac{\partial H}{\partial x^i}, \tag{43}$$

which enables one to derive also the two constants of motion

$$E = A(r)\frac{dt}{d\lambda}, \quad L = C(r)\frac{d\phi}{d\lambda}. \tag{44}$$

Preprints (www.preprints.org) | NOT PEER-REVIEWED | Posted: 19 August 2022 doi:10.20944/preprints202208.0354.v1

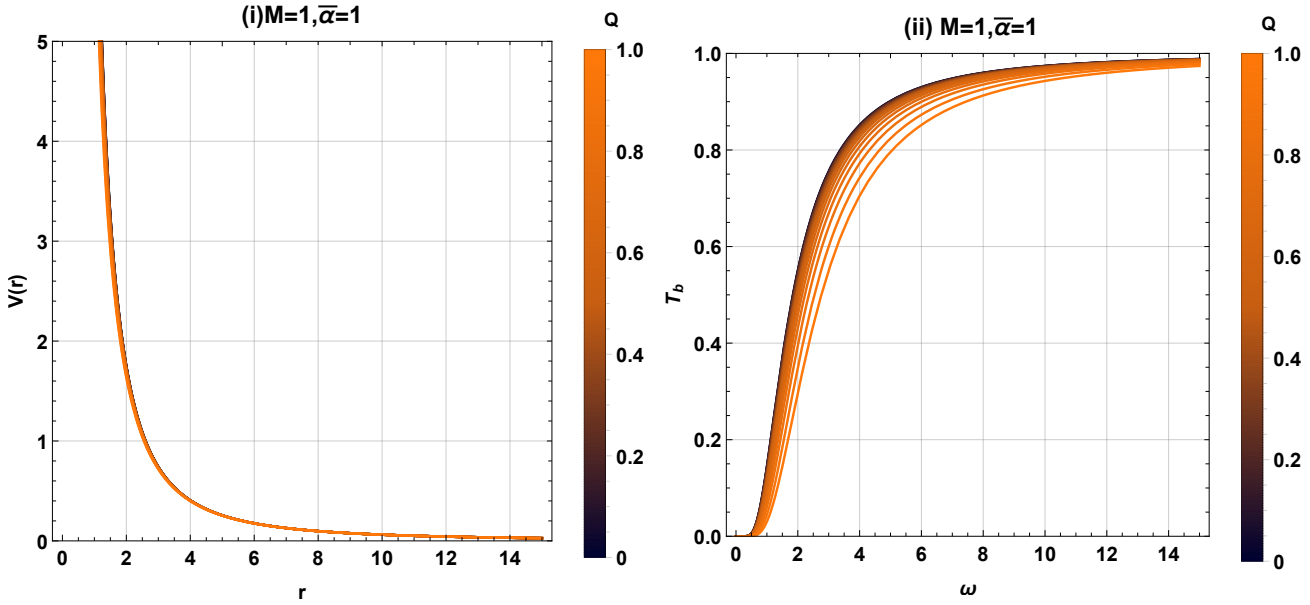

FIG. 5: The potential with $l = 2$ is shown in (i), and the corresponding bound of greybody factor of charged BH is shown in (ii).

It is useful to define the impact parameter:

$$b \equiv \frac{L}{E} = \frac{C(r)}{A(r)} \frac{d\phi}{dt}. \tag{45}$$

In the metric, $ds^2 = 0$ can also describe null geodesics, and using Eq. (44), we can derive the orbit equation as

$$\left(\frac{dr}{d\phi}\right)^2 = \frac{C(r)}{B(r)} \left(\frac{h(r)^2}{b^2} - 1\right), \tag{46}$$

where [110]

$$h(r)^2 = \frac{C(r)}{A(r)} n(r)^2 = \frac{C(r)}{A(r)} \left(1 - \frac{\omega_e^2}{\omega_0^2} A(r)\right), \tag{47}$$

if one assumes a non-gravitating and homogeneous plasma [111]. Note that it easily reduces to the Schwarzschild case if $n(r) = 0$. Next, the photonsphere radius can be determined if one evaluates $h'(r) = 0$ and solve r:

$$\left(\frac{\omega_e^2}{\omega_0^2} A(r)^2 - A(r)\right) C'(r) + C(r) A'(r) = 0. \tag{48}$$

Considering the metric function in Eq. (7), we can only determine the photonsphere radius, either affected by plasma or not, through numerical considerations. For instance, if $n(r) = 0$, the photonsphere radii can be found via

$$\bar{\alpha} M^4 Q^2 + \frac{15 M r^5}{2} - 5 Q^2 r^4 - \frac{5 r^6}{2} = 0. \tag{49}$$

Consider the black hole at O, then a static observer at a distance $r_{\rm obs}$ and $\theta_{\rm obs} = \pi/2$. A simple geometrical construction will define the shadow's angular radius as [110]

$$\tan(\alpha_{\rm sh}) = \lim_{\Delta x \to 0} \frac{\Delta y}{\Delta x} = \left(\frac{C(r)}{B(r)}\right)^{1/2} \frac{d\phi}{dr}\bigg|_{r=r_{\rm obs}}, \tag{50}$$

Preprints (www.preprints.org) | NOT PEER-REVIEWED | Posted: 19 August 2022 doi:10.20944/preprints202208.0354.v1

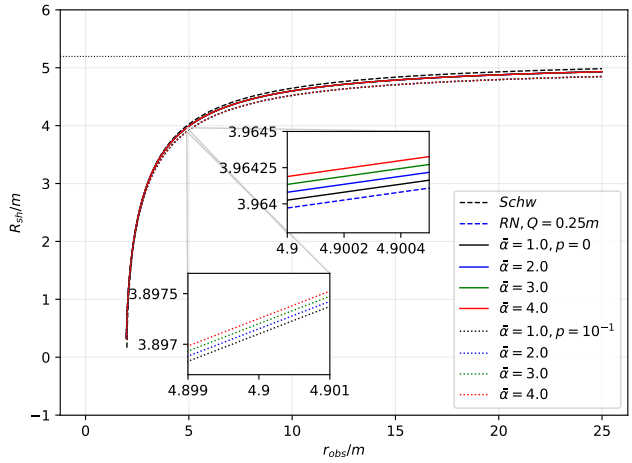

FIG. 6: Plot of the shadow radius for a charged black hole with NLED correction $\bar{\alpha}$ varies. The plot shows the cases where the BH is immersed or not in a plasma medium.

which simplifies to

$$\sin^2(\alpha_{\rm sh}) = \frac{b^2_{\rm crit}}{h(r_{\rm obs})^2}. \tag{51}$$

Here, the critical impact parameter can be derived from the orbit equation. That is, if we take $\frac{dr^2}{d^2\phi} = 0$ which, for our result, yields

$$b^2_{\rm crit} = -\frac{r^2_{\rm ph}\left[\bar{\alpha}M^4pQ^2 - 30Mpr^5_{\rm ph} + 10pQ^2r^4_{\rm ph} + 20(p-1)r^6_{\rm ph}\right]}{2\bar{\alpha}M^4Q^2 - 10Mr^5_{\rm ph} + 10r^6_{\rm ph}}, \tag{52}$$

where $p = \frac{\omega_e^2}{\omega_0^2}$. Then the shadow radius can be sought off as

$$R_{\rm sh} = \left\{-\frac{r^2_{\rm ph}\left[\bar{\alpha}M^4pQ^2 - 30Mpr^5_{\rm ph} + 10pQ^2r^4_{\rm ph} + 20(p-1)r^6_{\rm ph}\right]}{2\bar{\alpha}M^4Q^2 - 10Mr^5_{\rm ph} + 10r^6_{\rm ph}}\left(1 - \frac{2M}{r_{\rm obs}} + \frac{Q^2}{r^2_{\rm obs}} - \frac{\bar{\alpha}M^4Q^2}{10r^6_{\rm obs}}\right)\right\}^{1/2}. \tag{53}$$

The result of Eq. (53) is shown in Fig. 6, where we considered $p = 10^{-1}$. We also plotted the Schwarzschild and the RN cases for comparison. We observed how the shadow radius changed as the static observer increased its distance from the black hole. Near the horizon, we can see that the effect of $\bar{\alpha}$ is negligible since the differences are very small. The NLED correction begins to manifest around $r_{\rm obs} = 3M$ and greater. With how the curve behaves, we can say that it follows the general trend of the Schwarzschild case. For the RN case, the existence of the charge $Q = 0.25M$ decreases the shadow. When the NLED correction $\bar{\alpha}$ increases, its effect on the shadow is to increase it. Finally, when the plasma parameter p is considered, it decreases the shadow radius overall. These effects are quite small, even at $r_{\rm obs} \to \infty$ as hinted by the inset plot.

We close this section by considering the dark matter effect, as described by the index of refraction $n(\omega)$, to the shadow of the BH with NLED correction. Our calculation revealed that with this model for dark matter, the photonsphere radius remains independent to $n(\omega)$, and still can be found through Eq. (49). Then, we find the critical impact parameter to be dependent to $n(\omega)$:

$$b^2_{\rm crit} = \frac{10n(\omega)^2r^8_{\rm ph}}{\bar{\alpha}M^4Q^2 - 5Mr^5_{\rm ph} + 5r^6_{\rm ph}}, \tag{54}$$

which reveals that the shadow radius should be proportional to $n(\omega)$:

$$R_{\rm sh} = \left\{\frac{10n(\omega)^2r^8_{\rm ph}}{\bar{\alpha}M^4Q^2 - 5Mr^5_{\rm ph} + 5r^6_{\rm ph}}\left(1 - \frac{2M}{r_{\rm obs}} + \frac{Q^2}{r^2_{\rm obs}} - \frac{\bar{\alpha}M^4Q^2}{10r^6_{\rm obs}}\right)\right\}^{1/2}. \tag{55}$$

Preprints (www.preprints.org) | NOT PEER-REVIEWED | Posted: 19 August 2022 doi:10.20944/preprints202208.0354.v1

Indeed, this result shows that the dark matter astrophysical environment can affect the size of the shadow as photons travels through such medium form $r_{\rm ph}$ to $r_{\rm obs}$. Although $r_{\rm ph}$ remains unaffected by the dark matter medium, this is not the case for $R_{\rm sh}$.

IX. CONCLUSION

This research is based on the study of the charged BH within NLED by utilizing the Gibbons and Werner approach to calculate the deflection angle $\hat{\theta}$ in vacuum Eq. (20), plasma in Eq. (25), and DM in Eq. (28) mediums. The bending angle in these mediums is shown to be dependent on the mass M of a gravitating body, charge Q, dimensionless parameter $\bar{\alpha}$ and the impact parameter u.

In a plasma medium, we have obtained that the deflection angle in Eq. (25) depends on the plasma terms, and due to the plasma effect, the deflection angle is greater than the angle obtained in a vacuum. We also investigated that by reducing the photon frequency viewed by a static observer at infinity while keeping the electron plasma frequency constant, the bending angle in the plasma medium increases. In the case of DM medium, we examined that the effect of the DM increases the deflection angle of the charged BH.

In all the above mediums, it is worth noting that the bending angle $\hat{\theta}$ of a charged BH reduces to the bending angle of Reissner-Nordstrom BH when $\bar{\alpha} = 0$, and in the absence of Q, the angle reduces to the deflection angle of Schwarzschild BH up to the fourth order of M. Further, we have examined that by eliminating the plasma and DM terms, the deflection angle in Eq. (25) and Eq. ((28) reduces to the deflection angle in Eq. (20).

Moreover, we have analyzed the bending angle graphically in both vacuum and plasma mediums. For this purpose, we examined the bending angle $\hat{\theta}$ w.r.t the impact parameter u at the various values of Q. For $0 \leq Q \leq 1$, we have observed that at the small value of impact parameter u, the bending angle $\hat{\theta}$ is positive. The bending angle $\hat{\theta}$ approaches zero as the value of impact parameter u increases. We have also inspected that the bending angle $\hat{\theta}$ gets its maximum value and then exponentially decreases as the values of charge increase $Q \to 1$. It is observed that for $Q = 0$, the bending angle exponentially decreases and approaches zero, which is the case of Schwarzschild BH. Moreover, we have observed that the graphical behavior of the bending angle $\hat{\theta}$ is the same in plasma and non-plasma cases.

The Hawking temperature of the charged BH within NLED is calculated, and the resulting temperature satisfies the standard form of the Hawking Temperature ($T_H = \frac{f'(r_h)}{4\pi}$). The obtained Hawking temperature in Eq. (35) depends on the M, Q and $\bar{\alpha}$. By considering $\bar{\alpha} = 0$, one can get the Hawking temperature of the Reissner-Nordstrom BH and the expression of Schwarzschild BH's Hawking temperature by taking $Q = 0$.

Furthermore, we have computed the rigorous bond of the greybody factor of the charged BH within NLED and observed that the obtained bound in Eq. (41) depends on the M, Q and $\bar{\alpha}$. Assuming $\bar{\alpha} = 0$, one can also get the expression of Reissner-Nordstrom BH's greybody bound and Schwarzschild BH bound by taking $Q = 0$.

We have also investigated the potential's graphical behavior and bound off the greybody factor for $0 \leq Q \leq 1$ and $l = 0, 1, 2$. We have observed that for $l = 0$, the potential of the charged BH within NLED decreases and becomes zero as the value of r increases. On the other hand, the corresponding bound increases and remains 1 as far as ω approaches infinity. For $l = 1, 2$, we have observed that the potential exponentially decreases and approaches zero and the greybody factor bound shows the convergent behavior, which converges to 1.

Finally, we also explored the effects of NLED with or without plasma and the dark matter parameter $n(\omega)$ on the black hole's shadow radius. The NLED parameter $\bar{\alpha}$ enhances the shadow size relative to the RN case, and we believe this effect is the same for other values of Q. The plasma effect, however, is meant to decrease the shadow size considerably. We also do not see any deviation from the general trend as it is the same as the Schwarzschild case. Finally, we have also seen the difference between the plasma and dark matter cases. While the plasma can affect both the photonsphere and shadow radii, dark matter only affects the shadow size, and the photonsphere remains independent.

[1] K. Akiyama et al. (Event Horizon Telescope), Astrophys. J. Lett. **875**, L1,17 (2019).
[2] S. Vagnozzi, R. Roy, Y.-D. Tsai, and L. Visinelli (2022), 2205.07787.
[3] A. Allahyari, M. Khodadi, S. Vagnozzi, and D. F. Mota, JCAP **02**, 003 (2020), 1912.08231.
[4] B. L. Voydatch and N. T. Mione (2019), URL https://digitalcommons.wpi.edu/mqp-all/7062.
[5] A. T. Michal Zajaek (2019), URL 10.48550/arXiv.1904.04654.
[6] R. M. Wald, Phys. Rev. D **10**, 1680 (1974).
[7] J. Maldacena, J. High Energ. Phys. **79** (2021).
[8] S. Hawking, Nature (1974).
[9] S. W. Hawking, Commun. in Math. Phys. **43** (1975).
[10] G. W. Gibbons and S. W. Hawking, Phys. Rev. D **15**, 2738 (1977).
[11] W. G. Unruh, Phys. Rev. D **14**, 870 (1976).

Preprints (www.preprints.org) | NOT PEER-REVIEWED | Posted: 19 August 2022 doi:10.20944/preprints202208.0354.v1

[12] T. Damour and R. Ruffini, Phys. Rev. D **14**, 332 (1976).
[13] M. K. Parikh and F. Wilczek, Phys. Rev. Lett. **85**, 5042 (2000).
[14] K. Srinivasan and T. Padmanabhan, Phys. Rev. D **60**, 024007 (1999).
[15] C. W. Robson, L. Di Mauro Villari, and F. Biancalana, Phys. Rev. D **99**, 044042 (2019).
[16] Y.-P. Zhang, S.-W. Wei, and Y.-X. Liu, Physics Lett. B **810** (2020).
[17] A. Övgün and I. Sakalli, Ann. of Phys. **413**, 168071 (2020).
[18] S. I. Kruglov, Int. J. of Mod. Phys. A **33**, 1850023 (2018).
[19] S. Fernando, Gen. Relativ. Gravit. **37**, 461481 (2005).
[20] W. Kim and J. J. Oh, J. of the Korean Phys. Society **52**, 986 (2008).
[21] J. Escobedo, Master's Thesis, Uni. of Amsterdam **6** (2008).
[22] C. H. Fleming, Uni. of Maryland. Dept. of Phys., Tech. Rep (2005).
[23] P. Lange, thesis, Uppsala Universitet (2007).
[24] M. Visser, Phys. Rev. A **59**, 427 (1999).
[25] P. Boonserm and M. Visser, Phys. Rev. D **78**, 101502 (2008).
[26] P. Boonserm et al., J. of Mathematical Phys. **55** (2014).
[27] W. Javed, I. Hussain and A. Övgün, Eur. Phys. J. Plus **137** (2022).
[28] H. Treder and G. Jackisch., Astronomische Nachrichten **302(6)**, 275 (1981).
[29] E. F. Eiroa, G. E. Romero, and D. F. Torres, Phys. Rev. D **66**, 024010 (2002).
[30] C. R. Keeton, C. S. Kochanek, and E. E. Falco, The Astrophys. J. **509**, 561 (1998).
[31] M. Sharif and S. Iftikhar, Astrophys. Space Sci. **361**, 36 (2016).
[32] K. S. Virbhadra, D. Narasimha, and S. M. Chitre, Astron. Astrophys. **337**, 1 (1998).
[33] A. F. Zakharov, Int. J. of Mod. Phys. D **27**, 06 (2018).
[34] K. S. Virbhadra and G. F. R. Ellis, Phys. Rev. D **65**, 103004 (2002).
[35] A. Bhadra, Phys. Rev. D **67**, 103009 (2003).
[36] R. Whisker, Phys. Rev. D **71**, 064004 (2005).
[37] S. Chen and J. Jing, Phys. Rev. D **80**, 024036 (2009).
[38] E. F. Eiroa, G. E. Romero, and D. F. Torres, Phys. Rev. D **66**, 024010 (2002).
[39] J. J. Zhang, Ruanjing and S. Chen., Phys. Rev. D **95**, 064054 (2017).
[40] G. W. Gibbons, C. M. Warnick, and M. C. Werner, Class. Quantum Grav. **25**, 245009 (2008).
[41] G. W. Gibbons and M. C. Werner, Class. Quantum Grav. **25**, 235009 (2008).
[42] M. C. Werner, Gen. Relat. and Gravi. **44**, 3047 (2012).
[43] K. Jusufi, A. Övgün, and A. Banerjee, Phys. Rev. D **96**, 084036 (2017).
[44] K. Jusufi, M. C. Werner, A. Banerjee, and A. Övgün, Phys. Rev. D **95**, 104012 (2017).
[45] A. Övgün, Phys. Rev. D **99**, 104075 (2019).
[46] F. Q. Ming, L. Zhao, and Y. X. Liu., Phys. Rev. D **104**, 024033 (2021).
[47] A. Ishihara et al., Phys. Rev. D **94**, 084015 (2016).
[48] A. Övgün, G. Gyulchev, and K. Jusufi., Ann. of Phys. **406**, 152 (2019).
[49] W. Javed, R. Babar, and A. Övgün, Phys. Rev. D **100**, 104032 (2019).
[50] M. K. Z. Jafarzade, Khadije and F. S. Lobo., J. of Cosmo. Astropart. Phys. **04**, 008 (2021).
[51] K. Takizawa, T. Ono, and H. Asada, Phys. Rev. D **101**, 104032 (2020).
[52] M. Okyay and A. Övgün, JCAP **01**, 009 (2022), 2108.07766.
[53] H. E. Moumni, K. Masmar, and A. Övgün, Int.J.Geom.Meth.Mod.Phys. p. 2250094 (2022).
[54] W. Javed, J. Abbas, and A. Övgün, Ann. of Phys. **418**, 168183 (2020).
[55] S. Hensh et al., The Eur. Phys. J. C **79**, 533 (2019).
[56] W. Javed, M. Aqib, and A. Övgün, New Astron. **96**, 101827 (2022).
[57] W. Javed, S. Riaz, and A. Övgün, Universe **8**, 262 (2022), 2205.02229.
[58] W. Javed, M. Aqib, and A. Övgün, Phys. Lett. B **829**, 137114 (2022), 2204.07864.
[59] W. Javed, I. Hussain, and A. Övgün, Eur. Phys. J. Plus **137**, 148 (2022), 2201.09879.
[60] A. Övgün, Phys. Rev. D **98**, 044033 (2018), 1805.06296.
[61] Z. Li and A. Övgün, Phys. Rev. D **101**, 024040 (2020), 2001.02074.
[62] W. Javed, j. Abbas, and A. Övgün, Phys. Rev. D **100**, 044052 (2019), 1908.05241.
[63] Z. Li, G. Zhang, and A. Övgün, Phys. Rev. D **101**, 124058 (2020), 2006.13047.
[64] Y. Kumaran and A. Övgün, Chin. Phys. C **44**, 025101 (2020), 1905.11710.
[65] W. Javed, A. Hamza, and A. Övgün, Phys. Rev. D **101**, 103521 (2020), 2005.09464.
[66] A. Övgün and I. Sakallı, Class. Quant. Grav. **37**, 225003 (2020), 2005.00982.
[67] A. Övgün, Turk. J. Phys. **44**, 465 (2020), 2011.04423.
[68] R. C. Pantig and A. Övgün, Eur. Phys. J. C **82**, 391 (2022), 2201.03365.
[69] N. J. L. S. Lobos and R. C. Pantig (2022), 2208.00618.
[70] J. Rayimbaev, R. C. Pantig, A. Övgün, A. Abdujabbarov, and D. Demir (2022), 2206.06599.
[71] W. Javed, R. Babar, and A. Övgün, Phys. Rev. D **99**, 084012 (2019), 1903.11657.
[72] K. Jusufi and A. Övgün, Phys. Rev. D **97**, 024042 (2018), 1708.06725.
[73] A. Övgün, I. Sakallı, and J. Saavedra, JCAP **10**, 041 (2018), 1807.00388.
[74] K. Jusufi, M. C. Werner, A. Banerjee, and A. Övgün, Phys. Rev. D **95**, 104012 (2017), 1702.05600.
[75] I. Sakalli and A. Ovgun, EPL **118**, 60006 (2017), 1702.04636.

Preprints (www.preprints.org) | NOT PEER-REVIEWED | Posted: 19 August 2022 doi:10.20944/preprints202208.0354.v1

[76] F. Zwicky, The Astrophys. J. **86**, 217 (1937).
[77] G. Hinshaw et al. (WMAP Collaboration), The Astrophys. J. Supple. Ser. **208**, 19 (2013).
[78] J. L. Feng, The Astrophys. J. Supple. Ser. **48**, 495 (2010).
[79] D. C. Latimer, Phys. Rev. D **88**, 063517 (2013).
[80] O. A., Universe **5**, 115 (2019).
[81] R. C. Pantig and E. T. Rodulfo, Chin. J. Phys. **66**, 691 (2020).
[82] J. D. Jackson, 2nd Ed. Wiley, NY (1975).
[83] M. Born and L. Infeld., Proc. R. Soc. Lond. **144**, 425 (1934).
[84] E. Ayn-Beato and A. Garca., Phys. Lett. B **493**, 149 (2000).
[85] E. Ayon-Beato and A. Garca., Phys. Lett. B **464**, 25 (1999).
[86] Z.-Y. Fan and X. Wang, Phys. Rev. D **94**, 124027 (2016).
[87] S. Chinaglia and S. Z. ., Gen. Rela. and Gravi. **49**, 1 (2017).
[88] K. A. Bronnikov, Int. J. Mod. Phys. D **27**, 1841005. (2018).
[89] G. Crisnejo and E. Gallo, Phys. Rev. D **97**, 124016 (2018).
[90] H. J. Mosquera Cuesta, G. Lambiase, and J. P. Pereira, Phys. Rev. D **95**, 025011 (2017), 1701.00431.
[91] H. J. Mosquera Cuesta and G. Lambiase, JCAP **03**, 033 (2011), 1102.3092.
[92] H. J. Mosquera Cuesta and G. Lambiase, Phys. Rev. D **80**, 023013 (2009), 0907.3678.
[93] K. Akiyama et al. (Event Horizon Telescope), Astrophys. J. Lett. **930**, L12 (2022).
[94] J. L. Synge, **131**, 463466 (1966).
[95] J.-P. Luminet, **75**, 228 (1979).
[96] J. M. Bardeen, in *Les Houches Summer School of Theoretical Physics: Black Holes* (1973), pp. 215–240.
[97] G. Gyulchev et al., **2075**, 215240 (2019).
[98] G. Gyulchev et al., The European Physical Journal C **78**, 112 (2018).
[99] V. Perlick and O. Y. Tsupko, Phys. Rev. D **95**, 104003 (2017).
[100] R. C. Pantig and A. Övgün (2022), 2202.07404.
[101] R. C. Pantig, P. K. Yu, E. T. Rodulfo, and A. Övgün (2021), 2104.04304.
[102] R. A. Konoplya and A. Zhidenko, Astrophys. J. **933**, 166 (2022), 2202.02205.
[103] R. A. Konoplya, Phys. Lett. B **795**, 1 (2019), 1905.00064.
[104] Z. Xu, X. Hou, X. Gong, and J. Wang, JCAP **09**, 038 (2018).
[105] Z. Xu, X. Gong, and S.-N. Zhang, Phys. Rev. D **101**, 024029 (2020).
[106] K. Nomura, D. Yoshida, and J. Soda, Phys. Rev. D **101**, 124026 (2020), 2004.07560.
[107] K. Nomura and D. Yoshida, Phys. Rev. D **105**, 044006 (2022).
[108] G. S. Bisnovatyi-Kogan and O. Y. Tsupko, Universe **3**, 57 (2017).
[109] D. C. Latimer, Phys. Rev. D **88**, 063517 (2013).
[110] V. Perlick, O. Y. Tsupko, and G. S. Bisnovatyi-Kogan, Phys. Rev. D **92**, 104031 (2015).
[111] G. Crisnejo and E. Gallo, Physical Review D **97**, 124016 (2018).